Planning of distributed energy storage by a complex network approach

Journal of Renewable and Sustainable Energy

Planning of distributed energy storage by a complex network approach

Cite as: J. Renewable Sustainable Energy **14**, 024102 (2022); https://doi.org/10.1063/5.0087338
Submitted: 04 February 2022 • Accepted: 28 March 2022 • Published Online: 21 April 2022

Published open access through an agreement with Xi'an Jiaotong-Liverpool University Department of Electrical and Electronic Engineering

Qigang Wu, Fei Xue, Shaofeng Lu, et al.

Journal of Renewable and Sustainable Energy ARTICLE scitation.org/journal/rse

Planning of distributed energy storage by a complex network approach

Cite as: J. Renewable Sustainable Energy **14**, 024102 (2022); doi: 10.1063/5.0087338
Submitted: 4 February 2022 · Accepted: 28 March 2022 ·
Published Online: 21 April 2022

Qigang Wu,[1] Fei Xue,[2,a)] Shaofeng Lu,[3] Lin Jiang,[1] Xiaoliang Wang,[1] and Tao Huang[4]

AFFILIATIONS

[1]Department of Electrical Engineering and Electronics, University of Liverpool, Liverpool L69 3GJ, United Kingdom
[2]Department of Electrical and Electronic Engineering, Xi'an Jiaotong-Liverpool University, Suzhou 215123, China
[3]Shien-Ming Wu School of Intelligent Engineering, Guangzhou International Campus, South China University of Technology, Guangzhou, China
[4]Politecnico di Torino, Torino, Italy

[a)]Author to whom correspondence should be addressed: Fei.Xue@xjtlu.edu.cn

ABSTRACT

An energy storage system (ESS) has been considered one promising technology in dealing with challenges from the risk of power fluctuations and load mismatch in power girds. A distributed ESS (DESS) has better efficiency in reducing net losses and operating costs. The net-ability quantifies the power transmission ability across the grid where power is delivered from generators to loads under constraints. This paper proposes a new complex network-based metric: energy storage performance (ESP), for assessing the significance of the DESS inside a power grid. It aids the optimal location selections by improving grids' net-ability structurally. An auxiliary genetic algorithm (GA) sizing strategy is also deployed for deciding the optimal capacity of each DESS with the minimum daily operating and investment costs. The result shows that the DESS improves the rate of cost reduction within an equivalent 24-h daily operation. Moreover, this methodology finds quasi-optimal solutions with better feasibility and efficiency. The improvement of network performance by the DESS depends on its original structure. The result shows that with the assistance of siting plan by a complex network theory, the calculation efficiency improves and performs better in larger power grids. In the IEEE-30 test system, our solution is about 1/3 calculation time as the GA search. The quasi-optimal costs 1.8% more than the optimal searched by the GA. Meanwhile, the DESS can save more cost for networks with higher network-wide ESP value. In the IEEE-118 and IEEE-300 test systems, only the proposed hybrid-GA search can find a solution within a limited calculation time. Therefore, it could be promising in solving siting issues in the planning of smart grids.

I. INTRODUCTION

Due to the target of carbon emission reduction and carbon neutrality, renewable energy source (RES) penetration is increasing rapidly in recent years.[1] However, higher penetration of renewable energy will significantly increase the risk of power fluctuations and load mismatches, impacting power supply stability, reliability, and quality.[2] Moreover, electrical power systems transfer progressively from centralized control regimes to distributed control systems, increasing the complexity and uncertainty of power grids.[3] With materials technology development, an energy storage system (ESS) becomes a possible solution for solving these defects. The ESS stores electrical energy and releases it later when needed with a suitable operating strategy;[4] therefore, it has been applied in several applications, particularly for electrified transportation and utility applications in power grids such as load shifting, energy arbitrage, and primary frequency regulation.[5] Meanwhile, a distributed energy storage system (DESS) offers new solutions for power system planners. Compared with the conventional centralized ESS, the DESS can deploy energy resources closer to users. For a large transmission or distribution system with more operational constraints and marginal losses, the DESS has the potential to create more value locationally. It supplies (or stores) energy at locations where the power transmission is frequently congested.[6] Reference 7 discusses the impact of installing the DESS into a partitioned distribution network, which can improve the degree of self-sufficient in each cluster.

However, the capacity of the DESS is still constrained as the energy and power density are limited due to modern materials and

chemical technology. Meanwhile, the location of the DESS in the utility network affects net losses due to the lossy transmission line and complex topological connections, which increases the operating cost for the grid operator. Thus, an optimal allocation for DESS is essential while applying it to power grid operation. Many research pieces optimize DESS allocation to minimize its total cost inside the power grid such as investment, operating, and equipment renewal costs.[8,9] Some papers introduce optimization methods based on optimal power flow (OPF) with storage installation such as stochastic programming,[10] mixed integer linear programming,[11] genetic algorithm (GA),[12] or particle swarm optimization.[13] Yi *et al.*[10] denoted a two-level optimization structure for allocating DESSs and evaluating the dispatchability by Mixed-Integer Linear Programming (MILP) and benders decomposition. Similarly, Ref. 14 proposed a bi-level multi-objective optimization scheme for peak shaving and renewable energy compensation with the installation of the DESS. Reference 15 presented a near-optimal method for finding the minimum operating cost and daily storage investment under optimal location and sizing of DESSs by Unit Commitment. Ghofrani *et al.*[16] introduced a framework for the optimal placement of the DESS within a high wind penetrated power system. They applied a GA-enhanced, Hong's point estimation-based probabilistic optimal power flow (P-OPF) method to maximize wind power utilization over the scheduling period. Simulation results show that the DESS has better utilization efficiency and reliability than the centralized ESS. However, due to the non-convex power flow constraints and the integer operating status of the DESS, the determination of optimal locations and capacities for DESSs is a non-deterministic polynomial-time (NP) hard problem, which is not efficient for an extensive system.[17,18] Meanwhile, there is no direct metric for suggesting a proper amount of DESSs inside the power grid. Aside from that no previous works were aware that DESSs might improve the power grid performance to different extents due to various system structures and conditions. No metric has been introduced for assessing this difference as an inherent feature of different networks.

The complex network (CN) theory has been widely accepted as an impactful tool for analyzing power grids' structural features. It has been developed to be a popular field as it connects disciplines, including graph theory, probability and statistics, statistical mechanics, and control theory.[19] Many power network analysis applications are addressed with CN, such as assessment of robustness and vulnerability,[20] power grid resilience, and cascading failure analysis.[21,22] Nevertheless, most of these research works only consider the static topological aspects; structural approaches seldom discuss power flow dynamics and intra-hour relations inside the power network. DESS devices can operate under both charging and discharging modes, which is not considered a specific node type in previous works. The impact of the DESS on power grids' performance and stability has not been evaluated from the structural perspective. To the best of our knowledge, no works have been done to apply complex networks in DESS planning.

The contributions of this paper include:

(a) An index based on network topology analysis is introduced to evaluate the improvement of the network's performance when adding DESSs on different buses.
(b) We argue that the performance improvement of power grids by DESSs significantly depends on the original network structure.
(c) We propose that the number and sites of DESS-affiliated buses can be determined from a topological perspective. No paper has discussed how to decide the number of DESS-located buses by grid's topology and generator (and load) setup.
(d) We use the metric above as part of DESSs' optimal allocation, which accelerates the computational efficiency of the GA search.

Section II introduces the concept of energy storage performance (ESP) based on the idea of net-ability. Section III explains the optimization strategy for determining the optimal allocation of the DESS. In Sec. IV, simulation results are presented with a comparison between the pure heuristic algorithm and the proposed hybrid approach.

II. EVALUATION OF DESS PERFORMANCE BY STRUCTURE ANALYSIS

In this session, we propose a new metric, energy storage performance (ESP) for assessing the significance of the DESS equipped inside a specific power grid by the complex network theory. Moreover, the optimal location can be determined by ranking the ESP of different buses as well.

As illustrated in Fig. 1, we classify two main groups of factors for assessing the real-world power system operations: static and structural and dynamic factors. The static factors, such as the grid's topological connections or installed generator's capacity, are defined as permanently fixed parameters that cannot be changed during the whole power grid assessment procedure. It estimates the maximum ability to transfer power from generators to demands within the limitations of devices or transmission lines. On the other hand, the dynamic factors, including real-time load or quantity of intermittent energy in different periods, represent aspects that may change under different operating scenarios. Static factors constrain the network to operate within a reasonable domain, and dynamic factors determine how it works. However, with the integration of static and dynamic factors, the calculation complexity is expanded rapidly and inefficient for an extensive power network. Therefore, this paper will discuss a new metric that extracts static factors in power grids to evaluate transmission ability and efficiency improvement while integrating with DESS devices.

If a power grid is described as a graph, all buses, including generators, loads, or substations, are considered as nodes. Transmission lines are also represented as weighted or unweighted edges connecting nodes. The overall performance of a complex network system is defined by global efficiency.[23] It measures the effectiveness of the information flow in both weighted and unweighted networks.

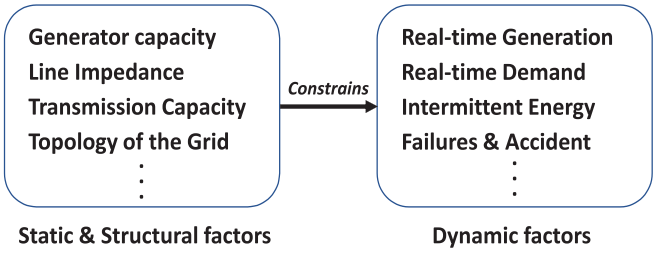

FIG. 1. Schematic of factors in power system operation. Static and structural factors constrain the real-time operation of the power system.

Pagani and Aiello[24] denoted that the efficiency of transferring electricity is one aspect for measuring the power grid's goodness from the topological point of view. An improved metric, net-ability, was designed to estimate the grid's performance.[20] It quantifies the ability of power transmission across the whole grid where power is delivered concurrently from generators to loads under grid operational security. Considering a network $Y(V, L)$, V is the set of vertices, which denote electric buses, and edges of the network, which symbolize power lines in the power grid, are represented as $L = \{l(i,j)\} \subset V \times V$. From the electrical system perspective, functional node type distribution can be summarized as three types: generator node $G = \{g_1, g_2, \ldots, g_{(N_G)}\} \subset V$, demand node $D = \{d_1, d_2, \ldots, d_{N_D}\} \subset V$ for absorbing energy from generators, and transmission node $T = V - (G \cup D)$, an intermediate point for connecting edges without any generation or consumption of energy. The original net-ability of network Y was defined as[25]

$$N(Y) = \frac{1}{N_G N_D} \sum_{g \in G} \sum_{\substack{d \in D \\ d \neq g}} \frac{C_g^d}{Z_d^g}, \tag{1}$$

where N_G and N_D are the number of generator and load buses. Z_g^d signifies the electrical distance between a generator-load pair $p(g,d) \in G \times D$. It implies the equivalent impedance between two nodes under the directionality of power flow[26] and is defined as

$$Z_g^d = \frac{U_g^d}{I_g} = z_{gg} - 2z_{gd} + z_{dd}, \tag{2}$$

where z_{gd} is the gth-row, dth-column element inside the impedance matrix of the power grid. Meanwhile, the equivalent topological transfer capability from generator node g to demand node d, C_g^d is described as follows:

$$C_g^d = \min_{l \in L} \left(\frac{C_l^{\text{cap}}}{|f_l^{gd}|} \right), \tag{3}$$

where C_l^{cap} is the active power transmission capacity across the line l. f_l^{gd} is the power transfer distribution factor (PTDF)[27] of line l, which indicates variations of active power in transmission lines due to the unit active power injected in node g and extracted from node d. However, with the integration of the DESS into the network, the DESS-located node cannot be defined only as a generator or load node since it has generator-load duality, which changes the node type distribution and results in mismatch for the net-ability. If the DESS is placed into a power grid, it becomes an intermediate point that temporarily stores the electricity from generator node(s) while charging mode and delivering power to load(s) under the discharging mode. Additionally, it is supposed that charging and discharging cannot be operated simultaneously.

An electrical circuit schematic for power transmission through an alternative route across the DESS is shown in Fig. 2. The interconnection between a generation-load pair g and d is simplified as equivalent impedance Z_{eq}; If the DESS is not added into the grid, power is transmitted directly through this interconnection. The maximum transmitted power without any constraints for the generator in this transmission mode is equal to the equivalent transmission capacity described in Eq. (3). However, if the DESS is placed into the network,

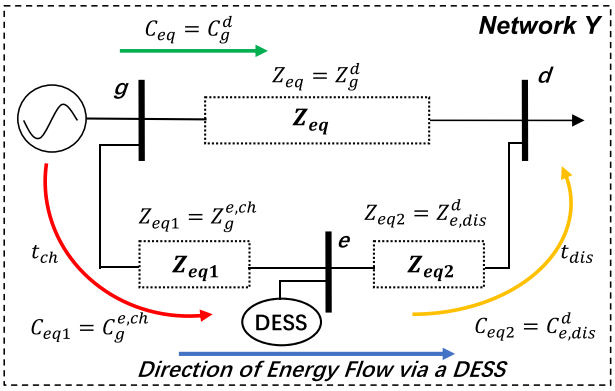

FIG. 2. Electrical circuit of the system with DESS. Power transmission has an alternative route via DESS with extra pesudo-time consumption t_{ch} and t_{dis}.

another route will be available for power flow. Power from the generator will be stored by the DESS temporarily and released when necessary. To explore the impact of the network structure on DESS performance, we assume that the generator-DESS pair's or DESS-load pair's transmission ability is constrained by the generator's or load's capacity and the topological transfer capability between the couple. The effect of the storage capacity itself is neglected in this stage. Therefore, the equivalent maximum transmission capacity from a generator g to a DESS bus e in the charging mode P_{ge}^{max} is

$$\begin{aligned} P_{ge}^{\max} &= \min(C_g^{e,\text{ch}}, P_g), \\ C_g^{e,\text{ch}} &= \min_{l \in L} \left(\frac{C_l^{\text{cap}}}{|f_l^{ge}|} \right). \end{aligned} \tag{4}$$

Meanwhile, the equivalent impedance between generator bus g and DESS-located bus e while DESS in the charging mode is

$$Z_g^{e,\text{ch}} = z_{gg} - 2z_{ge} + z_{ee}. \tag{5}$$

Similarly, the maximum transmitted power capacity between the DESS e and the demand d through the network is described as follows:

$$\begin{aligned} P_{ed}^{\max} &= \min(C_{e,\text{dis}}^d, P_d), \\ C_{e,\text{dis}}^d &= \min_{l \in L} \left(\frac{C_{ed,l}^{\text{cap}}}{|f_l^{ed}|} \right). \end{aligned} \tag{6}$$

The equivalent impedance between DESS bus e and load bus d is denoted as

$$Z_{e,\text{dis}}^d = z_{ee} - 2z_{ed} + z_{dd}. \tag{7}$$

As shown in Fig. 2, the equivalent impedance between g and d via DESS equals a series connection of $Z_g^{e,\text{ch}}$ and $Z_{e,\text{dis}}^d$, which is denoted as

$$Z_{ge}^{ed} = Z_g^{e,\text{ch}} + Z_{e,\text{dis}}^d. \tag{8}$$

Here, we propose a pseudo-time of consumption in the DESS node to demonstrate the DESS pseudo-operation under the static CN analysis. It aims at clarifying the asynchronism of charging and

discharging operations, which affects transmission efficiency. It is supposed that the quantity of shifted energy required by a load bus d through a storage bus e is Eng^{e}_{gd} and transmission losses are negligible. Moreover, it is assumed that transmission capabilities in the charging mode in Eq. (4) and the discharging mode in Eq. (6) are fully utilized. Henceforward, the pseudo-time of consumption for the charging and discharging processes are

$$t_{\mathrm{ch}} = \frac{Eng^{e}_{gd}}{P^{\max}_{ge}}, \qquad t_{\mathrm{dis}} = \frac{Eng^{e}_{gd}}{P^{\max}_{ed}}. \tag{9}$$

While the DESS is operating, the pseudo-time of consumption can be summed, as the delivered energy from a generator to the DESS and from the DESS to the load are identical. Thus, the equivalent transmission capability through the DESS from g to d is

$$P^{ed}_{ge} = \frac{Eng^{e}_{gd}}{t_{ch} + t_{dis}} = \frac{P^{\max}_{ge} \cdot P^{\max}_{ed}}{P^{\max}_{ge} + P^{\max}_{ed}}. \tag{10}$$

From Eq. (10), the equivalent capacity is irrelevant to the quantity of dispatched energy Eng^{e}_{gd}. Referring to the definition of net-ability, we then introduce a metric ESP for assessing the improvement of network efficiency by installing DESSs. The nodal energy storage performance (ESP_n) for bus e is defined as

$$ESP_n(e) = \frac{1}{N_G N_D} \sum_{\substack{p \subset P \\ g \neq d}} \frac{P^{ed}_{ge}}{Z^{ed}_{ge}}, \tag{11}$$

where $P = \{(g, d)\} = G \times D$ is the notation of all generator-load pairs. For a particular generator-load pair p, if a DESS is located on either load or generator buses, power will be transmitted directly between g or d and e. The power transmission between overlapped nodes is not through the network; therefore, it is not discussed in evaluating network features.

Afterwards, we can calculate the ESP_n for every node and rank these data for determining the priority of buses placing DESSs. It will accelerate the calculation procedure of DESS optimal capacities and location allocation as it decides locations in advance, reducing variables in the NP-hard allocation problem.

Moreover, the global network-wide energy storage performance (ESP_G) of the grid $Y(V, L)$ is defined as an average value over all buses in the entire network

$$ESP_G(Y) = \frac{1}{N_V} \sum_{e \in V} ESP_n(e), \tag{12}$$

where V is the set of all buses inside network Y and N_V is the number of buses inside the grid. The ESP_G is equivalent to an additive net-ability value, where it provides an alternative route for power flow through DESS(s). This index can evaluate network's global capability for improving power transmission performance by DESSs, which mainly depends on its static and structural characteristics, including the topological connection of networks and the parameters of lines, generators, and loads, but not DESS itself. Meanwhile, as discussed in the previous paragraph, the net-ability could also be described as energy transfer efficiency. The shifted electrical power between peak and off-peak periods can be transferred more efficiently through DESSs. Thereby, we can reveal the effectiveness of installing DESS in the network by the structural analysis. ESP_G can also compare DESS productivity among different networks without time-consuming optimal allocation.

III. OPTIMAL ALLOCATION STRATEGY OF DESS

The installation of DESS should improve power transmission efficiency by adjusting the spatial and temporal distribution of power flow. The *ESP* metric considers DESS's spatial contribution to offer a new route for power transmission between any generator-load pair through DESS. It avoids possible congestions in a power grid and improves the stability of the power grid. However, in an actual engineering application, the sizing of the DESS is also critical because of the trade-off between operating costs from generators and DESS investment costs.

Figure 3 illustrates the framework of the optimal allocation strategy for DESSs assigned in this paper. The DESS has three operating states: charge, discharge and idle. It can be expressed as a group of

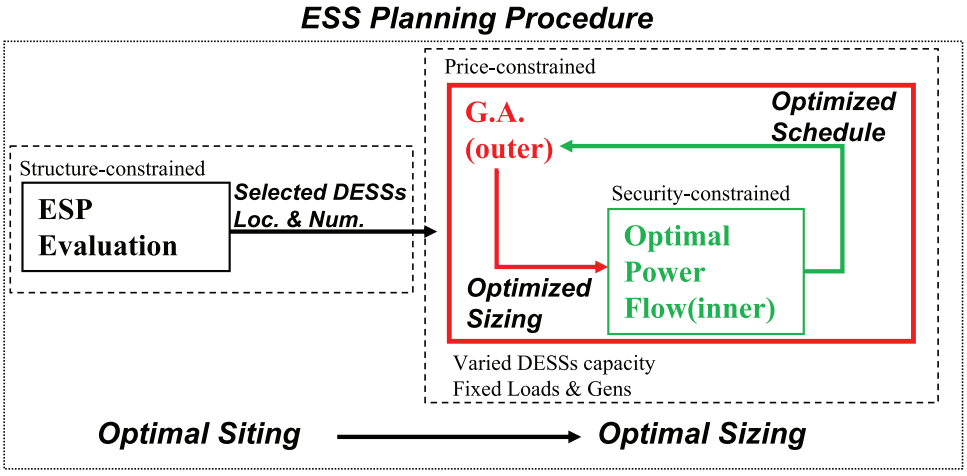

FIG. 3. Framework of optimal allocation of the DESS. ESP evaluation determines the DESS number and location, and the capacity is subsequently allocated by the hierarchical GA search.

integers. Meanwhile, the DESS's capacity is not continuous in engineering applications. The AC power flow is non-linear as well, which decides the actual power variation for DESSs. Therefore, the optimal allocation of the DESS is a mixed-integer non-linear problem. For this reason, we select the GA as the main optimization tool. The GA has good reliability during the calculation procedure. It can easily collaborate with existing models or integrate into hybrid approaches as well.[28,29] Meanwhile, the function can be easily transformed into the parallel implementation without restrictions on the program they process. However, the GA is a random search metaheuristic algorithm. If the number of variables is not limited, larger population sizes are necessary, which causes the iterations to be very slow. Henceforward, the decision is decomposed into a two-step model for reducing the complexity of the decision. First, the numbers of DESS-integrated buses and their locations are selected by $ESP_n(e)$ in the descending order. Afterwards, the size of each DESSs is determined by a hierarchical optimization model indicated in this section.

A. Optimal sizing of the DESS

In this part, the temporal contribution of the DESS is considered for minimizing the equivalent 24-h daily operating and fuel cost from generators and capital investment cost of DESSs. The objective function can be summarized as

$$f_{\text{obj.}} = \min\left\{ \underbrace{\sum_{s} f_s^{sc} \cdot \sum_{k=24} f_{\text{oper.}}[k]}_{\text{operating cost}} + \underbrace{\sum_{n\in\varepsilon} Co_n^{\text{inv}}}_{\text{DESS inv. cost}} \right\}, \tag{13}$$

where ε is the set of installed DESS variables, including DESS's location and capacity. $f_{oper.}$ represents the operating cost of devices during a single time interval. f_s^{sc} indicates the weight function for different load scenarios. The investment cost of the DESS is Co_n^{inv}. The objective function is a summation of the operating cost from generators, the replacement cost, and the investment cost from DESSs. We propose a bi-level hierarchical optimization model for determining the optimal sizing problem as it combines the consideration of economic and technical issues. The outer optimization model selects DESS capacity commitments by minimizing the sum of DESSs investment cost and the 24-h total operating cost from generators and DESSs. The inner layer optimization is designed for minimizing the total operating cost from all generators and DESSs within a specific period by adjusting the active power output of all dispatchable generators and DESS operations. The variables in this stage are active power outputs of dispatchable generators and DESSs operating states and power. Aside from that the capacity of the DESS is deterministic in this stage. The result of the inner optimization layer represents the optimized operating schedule for generators and DESSs under a particular combination of DESS allocations. In this paper, we choose multi-period AC-OPF as the inner optimization method and the GA as the outer optimization tool.

1. Outer optimization for DESS operation based on the genetic algorithm

This section introduces the tool for searching the optimal result of the objective function discussed before. The outer layer includes a selection method for the DESS capacity. The genetic algorithm is emerging as an efficient optimization method widely used to solve the non-linear, non-convex, and mixed-integer DESS placement.[16] This stage's primary work encodes the DESS optimal sizing problem into GA's chromosomes and defines the fitness function. The variable is equivalent to a gene, and it constitutes chromosomes. In the presented work, the fitness function is denoted as in Eq. (13).

The overall algorithm structure of the optimal allocation of the DESS is presented in Fig. 4. First, the optimal position is decided by the structural analysis methodology noticed in Sec. II. Then, the initial population in the GA is generated with random DESS(s) capacity. For every population generated by the GA, inner optimizations are calculated to evaluate each individual's fitness function. Meanwhile, the actual discharge or charge power of DESSs are determined by inner OPF, and the energy level for DESSs is updated simultaneously.

2. Inner optimization for DESS operation based on OPF

We propose AC-OPF as the optimization strategy in the inner layer. The internal optimization is to calculate the operating cost for the fitness function of the outer layer. First, a daily load leveling factor for all load buses is selected. The optimized output for each generator, including DESS, is calculated by the deterministic AC-OPF, subsequently. The charging or discharging of the DESS in each interval depends on the remaining energy level in the preceding interval; therefore, energy stored in the DESS is updated from the result simultaneously. The progress is repeated for 24 h, and the daily operating cost is assessed by summing the fuel cost within 24 h. Afterwards, this process will be repeated eight times to demonstrate eight scenarios where simulate the cost under weekdays or weekends in four seasons. For the deterministic AC optimal power flow, the objective function is

$$\begin{aligned} f_{obj.}^{inner} &= \min\{f_{oper.}\} = \min_{P,Q,V,\theta}\left\{\sum_{g\in G} f_p(P_g) + \sum_{n\in\varepsilon} f_{\text{rep}}(E_n)\right\} \\ &= \min\left\{\sum_{g\in G}(a_g P_g^2 + b_g P_g + c_g) + \sum_{n\in\varepsilon}(a_n \cdot P_n^{\text{DESS}})\right\} \\ &= \min\left\{\sum_{g\in G}(a_g P_g^2 + b_g P_g + c_g) + \sum_{n\in\varepsilon}\frac{1}{\Delta t}\frac{Co_{\text{rep}}^{\text{cap}}\cdot E_n}{LC\cdot E_n}\cdot P_n^{\text{DESS}}\right\}, \end{aligned} \tag{14}$$

where a_g, b_g, and c_g are the operating cost polynomial coefficient for generator g. P_n^{DESS} is the power input (or output) of the DESS in the charge (or discharge) mode. We suppose that the replacement cost of the DESS is part of the operating cost and is spread out into per unit of DESS charge (and discharge) energy. $Co_{\text{rep}}^{\text{cap}}$ is the capital replacement cost for a piece of DESS equipment, and the life cycle for this particular device is represented as LC. This function is subject to:

Equality constraints:

$$\begin{aligned} P_i &= P_{g_i} - P_{l_i} = \sum_{k=1}^{N_{bus}} V_i V_k [G_{ik}\cos\theta_{ik} + B_{ik}\sin\theta_{ik}], \\ Q_i &= Q_{g_i} - Q_{l_i} = \sum_{k=1}^{N_{bus}} V_i V_k [G_{ik}\sin\theta_{ik} + B_{ik}\cos\theta_{ik}]. \end{aligned} \tag{15}$$

Inequality constraints:

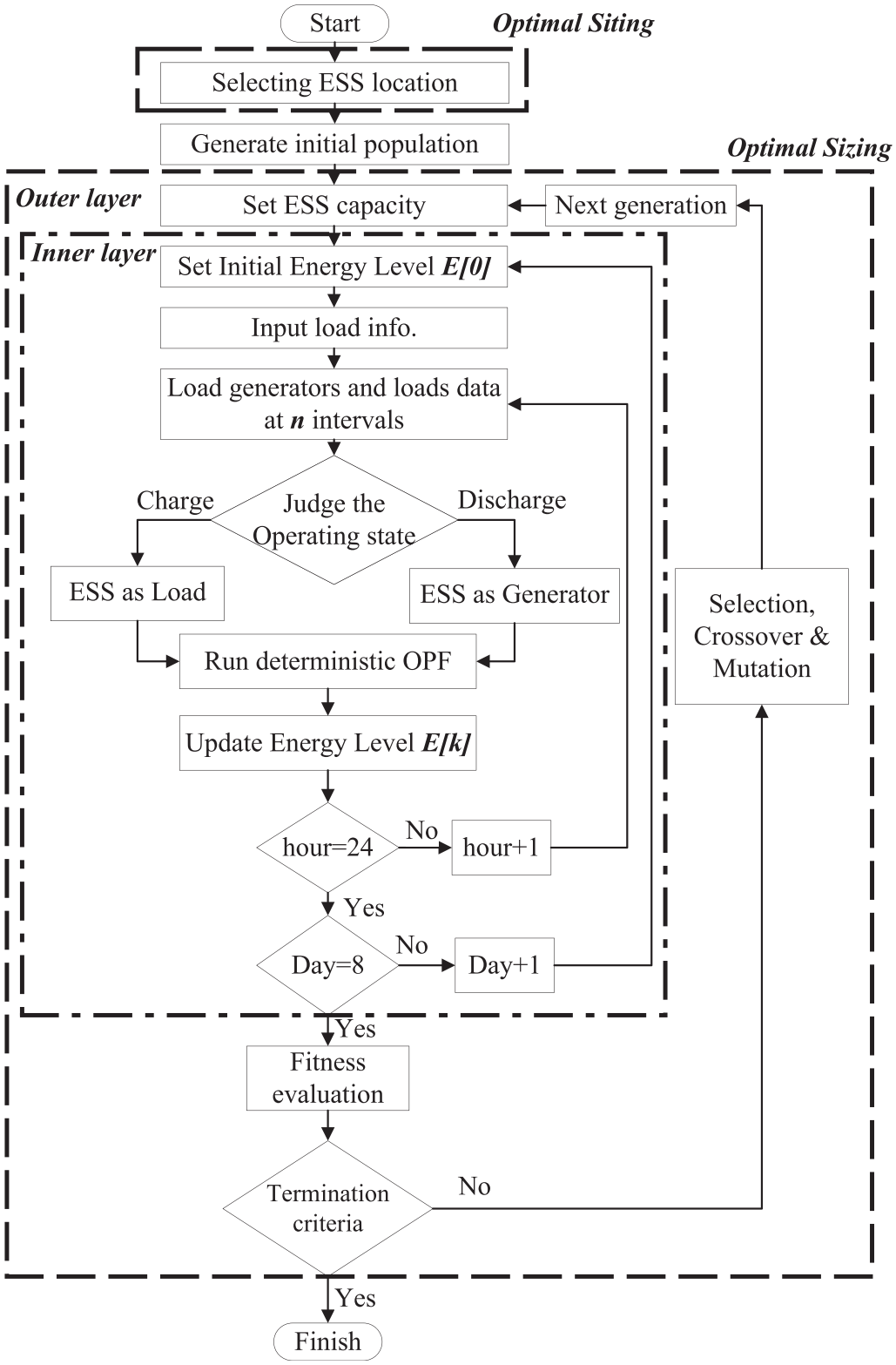

FIG. 4. The overall structure of optimal allocation of DESSs.

$$V_i^{\min} \le |V_i| \le V_i^{\max}, \tag{16}$$

$$S_l \le S_l^{\max}, \tag{17}$$

$$\begin{aligned} P_{g_i}^{\min} &\le P_{g_i} \le P_{g_i}^{\max}, \\ Q_{g_i}^{\min} &\le Q_{g_i} \le Q_{g_i}^{\max}. \end{aligned} \tag{18}$$

The equality constraints Eq. (15) represent the active and reactive power balancing for all nodes i in each time interval t. We assume that the DESS shifts active power from generators only without consuming or storing reactive power. The limitation for nodal voltage margin is described in Eq. (16). Line capacity for power flow is presented in Eq. (17). Equation (18) indicates active and reactive power generation limits for all generators.

The AC-OPF program can optimize the output of active and reactive power of each energy source individually, including generators and DESS in charge (as dispatchable load) or discharge (as generator) modes. In this paper, we suppose that the DESS does not participate in adjusting the reactive power; the balance of reactive power is supplied by generators only. Meanwhile, power output or input by the DESS is limited by constraints of charging and discharging power and stored energy level as well. The AC-OPF is implemented by an open-source MATLAB-based simulation package, MATPOWER.[30]

B. System description

For verifying the validity of the ESP metric, a power system integrated with DESS devices is modeled in this section. The fluctuation of demands within 24 h is considered in this model.

1. Load leveling factor modeling

The random model of loads inside the system is characterized as the Gaussian distribution with upper limits LR_{up} and lower limits LR_{lo}[16,31]

$$f_{LR}(lr) = \begin{cases} \dfrac{1}{\sqrt{2\pi\sigma^2}} \exp\left[-\dfrac{(lr-\mu)^2}{2\sigma^2}\right], & LR_{lo} \le lr \le LR_{up}, \\ 0, & lr < LR_{lo}, lr > LR_{lo}, \end{cases} \tag{19}$$

where lr represents the hourly demand leveling within target periods. Estimation of μ and σ values are based on the IEEE-RTS[32] system, which provides hourly, daily, and seasonally peak load in the percentage of nominal demands. Aside from that the load curves on weekdays and weekends are different. We select eight 24-h load-level scenarios under the varied weight f_s^{sc} in varied seasons and day types as listed in Table I. In each scenario, a 24-h load leveling factor is calculated for all load buses from Eq. (19).

2. Modeling of DESS

The purpose of DESS installation in this paper is for shifting the excess electric energy generated from generators into peak demand hours; otherwise, it will be mismatched, and the system cannot operate properly. The instantaneous energy balance in the DESS is discretized and described as

$$E_n[k] = E_n[k-1] + \left(\alpha \cdot \eta_n^c P_{n,c}[k] - \beta \cdot \frac{P_{n,d}[k]}{\eta_n^d}\right) \cdot \Delta t, \tag{20}$$

where $E_n[k]$ is the energy stored in the nth DESS unit at kth time interval and $E_n[k-1]$ represents the energy at the last interval, similarly. η_n^c and η_n^d are energy conversion coefficients in charge and discharge modes, respectively. α and β are the DESS charging or discharging status. Also, we suppose that the charging power $P_{n,c}[k]$ and discharging power $P_{n,d}[k]$ are constant during the time interval. Due to limitations of DESS's physical characteristics, the operation of the unit is constrained to

$$\text{SoC}_n^{\min} \le SoC_n[k] \le \text{SoC}_n^{\max}, \tag{21}$$

where $SoC_n[k]$ is the state-of-charge for the DESS at the kth interval as follows:

$$E_n[k] = SoC_n[k] \cdot E_n. \tag{22}$$

Based on the constraint of the energy level, the peak charging and discharging power within the interval k are constrained to

$$\begin{aligned} 0 \le P_{n,c}[k] &\le \min\left(P_{n,c}^{\max}, \frac{E_n \cdot \text{SoC}_n^{\max} - E_n[k-1]}{\eta_n^c}\right), \\ 0 \le P_{n,d}[k] &\le \min(P_{n,d}^{\max}, (E_n[k-1] - E_n \cdot \text{SoC}_n^{\min}) \cdot \eta_n^d), \end{aligned} \tag{23}$$

where the energy level at the end of each interval cannot exceed its limitations.

Our objective function is to minimize the equivalent 24-h daily cost, including ESSs capital cost, operating, and fuel costs from existing generators. Therefore, an economic analysis is established for integrating these costs. The energy capacity constraints DESS charge and discharge rate; thus, the apportioned daily installation investment cost of a DESS is

$$Co_n^{\text{inv}} = k_n^{\text{IRR}} \cdot Co_{\text{inv}}^{\text{cap.}} \cdot E_n, \tag{24}$$

where $Co_{\text{inv}}^{\text{cap.}}$ is the capital investment cost for the DESS. The capital cost factor k_n^{IRR} is defined by using the internal rate of return

$$k_n^{\text{IRR}} = \frac{1}{365} \frac{r_n(1+r_n)^y}{(1+r_n)^{y+1} - 1}, \tag{25}$$

where r_n represents the interest rate and y is the depreciation period. The primary purpose of the DESS is to time-shift the excess electric energy from generators to the peak demand period; therefore, the operating criteria are modeled as below

$$\begin{aligned} \alpha = 0, \beta = 1, &\quad \text{discharge state}, \\ \alpha = 1, \beta = 0, &\quad \text{charge state}. \end{aligned} \tag{26}$$

TABLE I. Weight of load-leveling in different scenarios.

	S1	S2	S3	S4	S5	S6	S7	S8
Season	Spring		Summer		Autumn		Winter	
Day-type	Wkd	Wknd	Wkd	Wknd	Wkd	Wknd	Wkd	Wknd
f_s^{sc}	5/28	2/28	5/28	2/28	5/28	2/28	5/28	2/28

IV. CASE STUDY

In this section, the proposed optimal allocation strategy of the DESS is tested on the IEEE-30 system under five cases to validate the ESP metric's effectiveness. The proposed ESP-GA hybrid method and the pure GA optimal allocation algorithm are compared in terms of calculation speed and accuracy. Subsection IV B simulates the multi-DESSs optimal allocation strategy proposed in this paper for the IEEE

30-bus, 118-bus, and 300-bus systems. MATPOWER is applied as the optimization tool for the inner OPF calculation, and MATLAB Global Optimization Toolbox implements the GA.

A. Evaluation of DESS in the IEEE-30 bus system under different circumstances

1. Description of test scenarios in IEEE-30 system

We distinguished the power grid operation factors into two parts: static and dynamic factors. The ESP is for measuring the effect from static factors. Therefore, we validate the ESP by discussing impacts from three static elements in the given IEEE-30 system in this part: (1) distributions of generator capacity P_g, (2) transmission capacity in different lines $C_{l,\text{Case III}}$, and (3) the topological connection in the power grid. Moreover, the hourly load-leveling, which belongs to dynamic factors, is also discussed in this test. Therefore, we design five scenarios by modifying the original IEEE-30 bus system and comparing the difference between them afterward. The summary of each case is listed as below:

I. Original IEEE-30 bus system.
II. Modifying each generator's capacity. The allocated capacities for each generator are identical.
III. Limiting maximum capacity for lines.
IV. Modifying the grid's structure. Three lines are removed, and four lines are installed.
V. Changing hourly load leveling in all nodes for every tested hour.

Table II enumerates the configuration for the testing system and differences in cases. Detailed modifications of case III and case IV are attached in Table III and Fig. 5. We suppose that the transmission line is "ideal" in case III. Modifications for line capacity cannot lead to changes in its impedance. For case V, a new set of load-leveling data is generated in Eq. (19) with an updated hourly peak total demand to 269.82 MW. The numbers of generators, total generation capacity, and total demand within every 24 h in eight typical days are static in all cases. The DESS planning in all five cases is performed by both the ESP-GA hybrid and pure GA methods. If there are no limitations for the DESS number, the pure GA method tends to allocate DESS on every bus. This is undoubtedly beneficial for system operation in theory, but it is not feasible in practical engineering. Therefore, in all five cases, both methods consider the allocation of three DESS devices. Each DESS device is possibly installed from bus 1 to bus 30.

2. Results and discussions for five cases

First, Table IV introduces the nodal ESP and network-wide ESP values in five testing cases. In case V, the hourly load leveling factor is

TABLE II. Configuration for IEEE-30. N_{DESS}, N_{gen}, and N_{branch} are the number of DESS, generators, and branches inside the IEEE-30 test system, respectively. The net demand in case V increases as the distribution of load-leveling in different buses changes.

N_{DESS}	N_{gen}	N_{branch}	$\sum P_{gen,\max}[k]$	$\sum P_{load,\max}[k]$
3	6	41	250.0 MW	269.8 MW (case V) 265.7 MW (others)

TABLE III. Configuration for case III modification. Line's capacity in case III is limited individually.

Branch no.	$C^{\text{cap}}_{l,\text{Case III}}$ (MW)	$C^{\text{cap}}_{l,\text{orig}}$ (MW)
1, 2, 4, 5, 9	130	973
7	90	
8	70	
3, 6, 11, 13, 14, 15, 16, 36	65	
10, 12, 17, 18, 19, 24, 25, 26, 27, 28, 29, 40, 41	32	
Others	16	

modified only, and there are no changes in the grid's topological connection, generator capacity and location, and demand leveling; therefore, it has the same ESP_G performance as case I. The performance in case III is similar to case I as well. The limitation constrains less power flow from transmission lines. With the modification for allocations of generators' capacity, case II achieves the best ESP_G score as the distribution of generation is more balanced than the original case. Figure 6 illustrates the value of ESP_n in two selected cases: case I and case IV. Bars with red color represent the pre-selected buses where DESSs will be located in further analysis. Initially, in bus 1, two lines are connected with the affiliation of a generator with the largest capacity. The nodal performance ESP_n in bus 1 can achieve a higher rank in case I. However, with the modification of lines connection, the number of lines to bus 1 is reduced to one. Therefore, the increase in the electrical distance between bus 1 and other generation buses and load buses eventually cuts transmission efficiency. As a result, the value of ESP_n falls in case IV because of higher losses of power transmission between bus 1 and other buses compared with case I. Conversely, for some nodes, e.g., bus 27 and bus 30, connecting more lines leads to a reduction in electrical distances, which results in better score of ESP_n. The detailed settings of the DESS are listed in Table V. The only difference between DESSs is its installed capacity. Other parameters, such as the

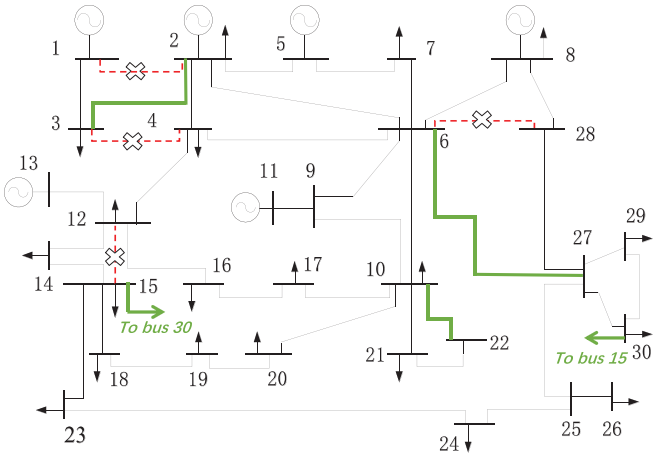

FIG. 5. Schematic for the IEEE-30 test system. Dashed red lines (removed) and solid green lines (added) are modifications in case IV. A transmission line between bus 15 and bus 30 is added in case IV.

TABLE IV. ESP result in the IEEE-30 system. $ESP_n(e)$ rank shows the descending order of the value of nodal ESP_n.

Case	Modification	$ESP_G(Y)$	$ESP_n(e)$ Rank	$ESP_{n,\max}$
I	None	25.42	2,1,8,4	87.66
II	Generator capacity	31.37	2,1,8,5	103.1
III	Line capacity	25.05	2,1,8,4	86.42
IV	Line connection	23.57	2,5,8,4	70.31
V	Load leveling	25.42	2,1,8,4	87.66

charging or discharging efficiency, are the same. The operation strategy of the DESS is for peak-shaving, where it discharges when the generation is insufficient within an interval and charges or idle in remaining periods. Table VI shows the result of DESS allocated locations and capacities using the hybrid ESP-GA method and the pure GA method. For example, in case I, two DESSs are located in bus 1 by the GA-only algorithm with the capacity of 20 and 8 MWh, respectively. Overall, all factors, including the structural, static and dynamic factors discussed in this case, could affect the 24-h total costs. The balanced generator distribution stated in case II shows the best economic efficiency in all cases and minimum DESS installation. Moreover, modifications in the static factors tested in case II and case IV can affect the results. The most significant deviation of daily cost and installed capacities of DESS occurred in case IV. The correctness of pre-defined location by the ESP metric is acceptable as well. Bus 2 inside the IEEE-30 bus systems receives the highest nodal *ESP* values in all five cases, and more DESS capacities are allocated on this bus.

The result in Table VI proves that the cost-efficiency of the entire network operation is increased with higher value of ESP_G. The ESP metric is developed from the concept of complex network efficiency and net-ability. It represents the power grid's performance and energy transfer efficiency measured by the complex network theory.

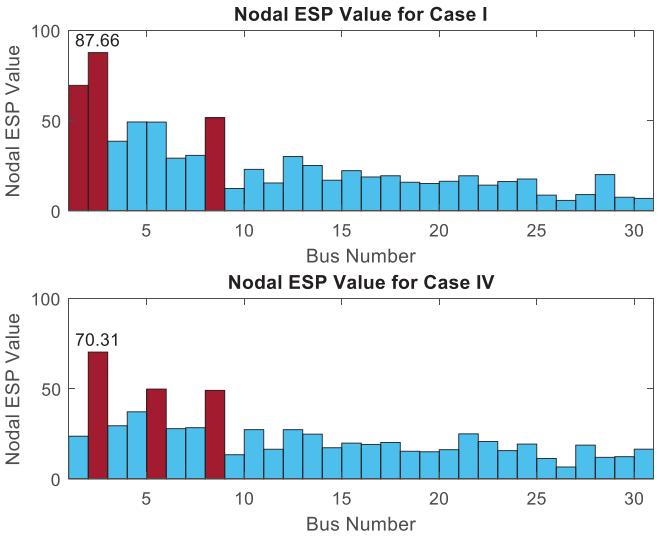

FIG. 6. The nodal ESP value in cases I and IV. Highlighted red bars represent better ESP value in these buses and are selected as DESS-installed locations.

TABLE V. Parameters for the DESS configuration used in this paper.

SoC^{max}	η_n^c	LC/cycles	Co_{inv}^{cap} ($/MWh)	Y/yrs
0.9	90%	1000	53 000	20
SoC^{min}	η_n^d	Minimum units	Co_{rep}^{cap} ($/MWh)	rn
0.1	95%	1 MWh	40 000	10%

Thus, higher ESP_G improves the energy delivery productivity with the integration of the DESS system.

Finally, as illustrated in Fig. 4, DESS optimal allocation calculation steps are similar between the hybrid ESP-GA and the pure GA search. Therefore, we compare the converged generation as a proof of calculation efficiency. The seventh column represents the converged generations in GA, which displays the calculation efficiency between the conventional GA and ESP-GA hybrid methods. The calculation efficiency is improved with less growth in the 24-h total costs between ESP-GA hybrid searching and the pure GA method for every case. The most considerable cost sacrifice occurs in case V with a loss of 1.80%. In conclusion, the CN-based ESP solution can accelerate the calculation time by per-defining the location of the DESS. Meanwhile, the DESS has better performance and saves more cost for networks with higher network-wide ESP.

B. DESS allocation in different systems

In this part, the effectiveness of the network-wide ESP_G metric and the calculation efficiency of DESS allocation are discussed between the ESP-GA hybrid searching method and GA-only for the IEEE 30-bus, 118-bus, and 300-bus testing systems. Table VII and Fig. 7 illustrate the value of numerical ESP in different systems. The first column represents the selection criterion for buses to install DESS (leveling ratio of maximum nodal ESP values in the tested system). The allocation strategy for DESS with the simultaneous analysis for optimal locations and capacities is an NP-hard problem.[17] The computation complexity is increased rapidly with the increment of the system scale. Therefore, we make a trade-off between the computation efficiency and global accuracy for the optimal allocation strategy of DESSs in the

TABLE VI. Results of the tested system. Numbers inside the brackets mean that these DESSs are located inside the same bus, and they could be merged as a single unit in later analysis.

Cases	Method	Location	Capacity	Total	ESP_G	Con. gen	Cost (10^5)
I	Hybrid	2,1,8	18,3,54	75	25.42	31	2.04
	GA	3,(1,1)	48,(20,8)	76		94	2.03
II	Hybrid	2,1,8	5,10,43	58	31.39	33	1.96
	GA	(1,1),2	(17,23),19	59		91	1.95
III	Hybrid	2,1,8	17,4,54	74	25.05	36	2.04
	GA	(1,1),2	(13,30),34	77		71	2.02
IV	Hybrid	2,5,8	1,40,83	124	23.57	28	2.23
	GA	5,(4,4)	88,(17,18)	123		116	2.22
V	Hybrid	2,1,8	70,12,5	87	25.42	30	2.20
	GA	2,(1,1)	80,(1,1)	82		103	2.16

TABLE VII. Ranking of nodal ESP in different cases. The first column means the percentile of the nodal ESP value. For example, four buses (bus no. 49, 65, 66, 80) have better ESP_n values in the 95th percentile.

%	IEEE-30	IEEE-118	IEEE-300
>95	2	49,65,66,80	3,7,130
>90	2	49,65,66,80,69	3,7,130,137,187,133
>85	2	(11 buses)	(22 buses)
>80	2	(20 buses)	(42 buses)
>75	2,1	(29 buses)	(59 buses)

following analysis. The number of installed DESS is decided where the nodal ESP value in its locations is over 90% of the maximum ESP value, as indicated by the first column of Table VII. For example, in the 300-bus system, the value of ESP_n in bus 133 is 114.78, where it is 90.19% of ESP_n in bus 3 ($ESP_n = 126.6$).

Henceforward, the number of DESSs installed in the 30-bus, 118-bus, and 300-bus systems is 3, 5, and 6, respectively. The summary of network configurations in three cases is listed in Table VIII. DESS charging and discharging coefficient is the same as Table V. The population size, mutation rate, and other GA settings are the same in both ESP-GA hybrid and pure GA methods. Table IX reveals the numerical results of the DESS allocations for two methods. It is clear that with the increasing number of DESS installed locations, more generations in the GA search are required in both ESP-GA hybrid and GA searching methods. The maximum number of generations of both methods is set as 150. In the IEEE-118 and IEEE-300 test systems, the pure GA searching method cannot find solutions within the maximum generation numbers. For a single 24-h AC-OPF inner-layer optimization, more time is consumed by increasing the case size. With assistance from ESP pre-defined locations, the search space is limited, resulting in a rapid acceleration of the calculation procedure with appropriate

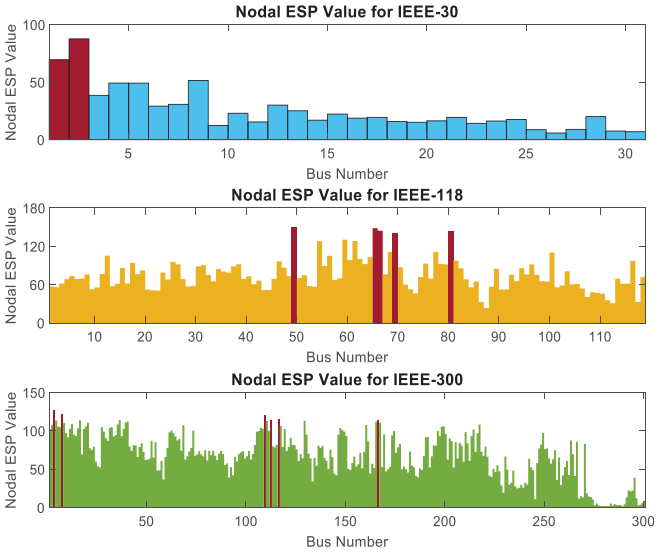

FIG. 7. The Nodal ESP Value in case 30, 118, and 300. Highlighted red bars represent better ESP value in these buses and are selected as DESS-installed locations.

TABLE VIII. Overall configuration and network-wide *ESP* value of IEEE 30, IEEE-118, and IEEE-300 bus system.

Sys.	$\sum P_{gen,\max}[k]$	$\sum P_{load,\max}[k]$	$ESP_G(Y)$
30	250.00	265.67	25.42
118	3592.3	3987.8	75.56
300	21 786	22 569	67.06

sacrifice in calculation accuracy. A set of quasi-optimal results could be found in a more extensive system restricting calculation times.

C. Discussion of ESP-GA hybrid method

In Sec. IV B, we have focused on applying the ESP metric for DESS allocation under different cases. The hybrid ESP-GA search can split the DESS allocation into two individual sub-problems and perform well in a large-scale system. This part will discuss the calculation efficiency of the ESP-GA method. Meanwhile, we evaluate the cost performance of the ESP-GA method by comparing the cost between different DESS locations sorted by the nodal ESP value. The program is run at Intel Core i5–6500 quad-core@3.2 GHz, 8G RAM, and MATLAB 2018b.

Table X records the computation time of ESP_n and GA search. Referring to the flow chart of DESS allocation strategy in Fig. 4, pure GA search and hybrid GA-ESP have similar structures at the stage of optimal cost evaluation. GA-ESP has fewer variables as it determines the location of DESS in advance, leading to a reduction in computation duty than the pure GA search. For example, in the 30-bus system, the nodal ESP_n value calculation time, which decides the preferred location of DESS, is 0.544 s. The calculation time for GA in each generation is up to 666.61 s. Table IX shows that the hybrid-GA search has 63 fewer converged generations than the pure GA search. With a quick DESS location evaluation computation, ESP-GA search significantly reduces the calculating time.

Table XI shows the cost efficiency of DESS allocation in different locations. We sorted the nodal ESP value in the ascending order and selected the same number of buses as the "best" case displayed in Table IX, where is named as "worst" case listed in the second column. The result indicates that in all cases, including IEEE-30 under different modifications, IEEE-118 and IEEE-300 test system, the total cost increases while DESSs located in nodes with less ESP_n values. As the operating states, such as generator distribution and hourly load, are the same inside one targeted test case, the DESS has a worse ability for adjusting the quantity of power flow between generator-load pairs, resulting in more power losses during the transmission. Meanwhile, a more significant gap of ESP value leads to more increment of the total cost. For example, the ratio of total ESP_n between the best and the worst scenario shows that there is the most significant difference in the 300-bus system. Referring to the 300-bus system schematic[33] selected nodes with the least value of ESP_n are located at the sub-distribution-network with a point of common coupling (PCC) at bus 39. Interactions between nodes chosen and the main grid, including the quantity of power exchange and the equivalent line impedance, are worse than nodes designated by the better ESP_n value. Moreover, the installed capacity of the DESS in the worst condition can also prove

TABLE IX. Result of DESS rating in IEEE-30, 118, and 300 bus system. Numbers inside the brackets mean that these DESSs are located inside the same bus, and they could be merged as a single unit in later analysis. The pure GA algorithm is not converged in IEEE-118 and IEEE-300 bus system within preset maximum generations.

System	Method	Location	Capacity	Total	ESP_G	Con. gen	Cost (10^5)
30	Hybrid	2,1,8	18,3,54	75	25.42	31	2.04
	GA	3,(1,1)	48,(20,8)	76		94	2.03
118	Hybrid	49,65,66,80,69	157,170,73,178,8	1043	75.56	88	17.2
	GA	N/A (exceed maximum generation)					
300	Hybrid	3,7,130,137,187,133	283,311,54,317,105,1903	2973	67.07	147	83.6
	GA	N/A (exceed maximum generation)					

TABLE X. Computing time of ESP_n and GA in IEEE-30, IEEE-118, and IEEE-300 cases. The third column records the averaged time consumption in the GA search method per generation. The computer specification is Core I5-6500 4-core@3.2 GHz, 8G RAM, MATLAB 2018b. Unit in this table is second.

Sys.	ESP_n (s)	GA/generation(s)
30	0.544	666.61
118	465.23	1480.9
300	21086	7699.2

that the choice of location is not appropriate. The total capacity of the DESS is 18 MWh, which is much smaller than its networkwide generation and demand. DESSs in these nodes are not very involved in adjusting the power flow distribution. The redundant capacity of the DESS in an improper position increases the total cost only without any hourly operating cost improvement and is optimized by GA afterwards. In conclusion, the DESS performance efficiency can be evaluated quickly by sorting the value of nodal ESP.

V. CONCLUSIONS

A network-structure-analysis based methodology for optimal siting of the distributed ESS is presented in this paper. It provides a new complex-network-based solution for determining the location of DESSs without heavy computation from optimization tools. Compared to the node types defined initially in complex networks, we propose a new bus type for reflecting the spatial operations of a storage element inside the power grid. Then, a new metric ESP is defined with the comprehensive consideration of the structure and static factors that affect power grid operation. It integrates a new type storage bus and the structural net-ability features. The locations of DESSs can be selected by the ranked nodal ESP_n in the descending order. This metric can determine the number and locations of DESS-affiliated buses. Meanwhile, a network-wide global metric ESP_G is also suggested for evaluating the network inherent ability in utilizing DESS. The simulation results in IEEE-30 with five different scenarios show that modification of the network structure has the most significant impacts on ESP_G. With higher ESP_G in different cases, the power grid's DESS utilization efficiency enforces, resulting in the equivalent 24-h daily total cost decrement. Improvement of network performance by the DESS

TABLE XI. Result of DESS allocation in IEEE-30, 118, and 300 bus system with different pre-defined locations. The searching method of all cases is by the ESP-GA hybrid search. We select nodes with ESP_n value in the ascending and descending orders as the "best condition" and "worst condition." The fifth column represents the total value of the nodal ESP_n value. The ratio between the highest and lowest total ESP values is recorded in the seventh column. In the last column, it represents the percentage of cost increment than the best scenario.

Case	Condition		Location	DESS capacity	$\sum ESP_n$	Cost (10^5)	B/W $\sum ESP_n$	Cost increment
		Best	2,1,8	18,3,54	208.75	2.04		
	I	Worst	26,30,29	20,32,20	20.32	2.26	10.28	10.54%
		Best	2,1,8	5,10,43	251.22	1.96		
	II	Worst	26,30,29	15,26,15	25.22	2.16	9.96	10.20%
		Best	2,1,8	17,4,54	205.93	2.04		
30	III	Worst	26,30,29	20,31,20	17.65	2.26	11.66	10.78%
		Best	2,5,8	1,40,83	169.21	2.23		
	IV	Worst	26,25,28	4,90,28	30.03	2.41	5.63	8.24%
		Best	2,1,8	70,12,5	208.75	2.20		
	V	Worst	26,30,29	29,23,24	20.32	2.30	10.28	4.41%
		Best	49,65,66,80,69	157,170,73,178,8	726.61	17.20		
IEEE-118		Worst	87,112,86,117,111	4,63,7,3,32	155.72	17.69	4.67	2.83%
		Best	3,7,130,137,187,133	283,311,54,317,105,1903	712.90	83.61		
IEEE-300		Worst	9042,9025,9026,9032,9033,9031	5,2,5,3,1,2	11.56	106.6	61.65	27.51%

depends on the original structure of the network and the relationship between supply and demand. Furthermore, a comparative evaluation between GA searching and ESP-GA hybrid searching is performed to assess all tested systems' computational efficiency and accuracy. The result indicates that the new hybrid search strategy is more time-effective than the GA siting and sizing search with less growth of the daily cost reduction rate. The result suggests that ESP can efficiently find quasi-optimal locations for ESS. Based on this work, we may expect that the complex network theory could contribute much more in planning smart grids by solving siting issues.

ACKNOWLEDGMENTS

This work was supported in part by the Research Development Fund (Nos. RDF-15-02-14 and RDF-18-01-04) of Xi'an Jiaotong-Liverpool University and in part by the National Natural Science Foundation of China (No. 51877181).

AUTHOR DECLARATIONS

Conflict of Interest

The authors have no conflicts to disclose.

DATA AVAILABILITY

The data that support the findings of this study are available from the corresponding author upon reasonable request.

REFERENCES

[1]N. Zhang, H. Jiang, Y. Li, P. Yong, M. Li, H. Zhu, S. Ci, and C. Kang, "Aggregating distributed energy storage: Cloud-based flexibility services from China," IEEE Power Energy Mag. **19**, 63–73 (2021).
[2]S. X. Chen, H. B. Gooi, and M. Q. Wang, "Sizing of energy storage for micro-grids," IEEE Trans. Smart Grid **3**, 142–151 (2012).
[3]F. Katiraei, R. Iravani, N. Hatziargyriou, and A. Dimeas, "Microgrids management," IEEE Power Energy Mag. **6**, 54–65 (2008).
[4]S. Vazquez, S. M. Lukic, E. Galvan, L. G. Franquelo, and J. M. Carrasco, "Energy storage systems for transport and grid applications," IEEE Trans. Ind. Electron. **57**, 3881–3895 (2010).
[5]M. J. O'Malley, M. B. Anwar, S. Heinen, T. Kober, J. Mccalley, M. Mcpherson, M. Muratori, A. Orths, M. Ruth, T. J. Schmidt, and A. Tuohy, "Multicarrier energy systems: Shaping our energy future," Proc. IEEE **108**, 1437–1456 (2020).
[6]S. P. Burger, J. D. Jenkins, S. C. Huntington, and I. J. Perez-Arriaga, "Why distributed?: A critical review of the tradeoffs between centralized and decentralized resources," IEEE Power Energy Mag. **17**, 16–24 (2019).
[7]D. Hu, M. Ding, R. Bi, X. Liu, and X. Rong, "Sizing and placement of distributed generation and energy storage for a large-scale distribution network employing cluster partitioning," J. Renewable Sustainable Energy **10**, 025301 (2018).
[8]S. A. Bozorgavari, J. Aghaei, S. Pirouzi, A. Nikoobakht, H. Farahmand, and M. Korpås, "Robust planning of distributed battery energy storage systems in flexible smart distribution networks: A comprehensive study," Renewable Sustainable Energy Rev. **123**, 109739 (2020).
[9]M. Hannan, M. Faisal, P. Jern Ker, R. Begum, Z. Dong, and C. Zhang, "Review of optimal methods and algorithms for sizing energy storage systems to achieve decarbonization in microgrid applications," Renewable Sust. Energy Rev. **131**, 110022 (2020).
[10]J. H. Yi, R. Cherkaoui, and M. Paolone, "Optimal allocation of ESSs in active distribution networks to achieve their dispatchability," IEEE Trans. Power Syst. **36**, 2068–2081 (2021).
[11]Y. M. Atwa and E. F. El-Saadany, "Optimal allocation of ess in distribution systems with a high penetration of wind energy," IEEE Trans. Power Syst. **25**, 1815–1822 (2010).
[12]G. Carpinelli, G. Celli, S. Mocci, F. Mottola, F. Pilo, and D. Proto, "Optimal integration of distributed energy storage devices in smart grids," IEEE Trans. Smart Grid **4**, 985–995 (2013).
[13]M. Sedghi, M. Aliakbar-Golkar, and M. R. Haghifam, "Distribution network expansion considering distributed generation and storage units using modified pso algorithm," Int. J. Electr. Power Energy Syst. **52**, 221–230 (2013).
[14]J. Liu, H. Cheng, Y. Tian, P. Zeng, and L. Yao, "Multi-objective bi-level planning of active distribution networks considering network transfer capability and dispersed energy storage systems," J. Renewable Sustainable Energy **10**, 015501 (2018).
[15]H. Pandzic, Y. S. Wang, T. Qiu, Y. Dvorkin, and D. S. Kirschen, "Near-optimal method for siting and sizing of distributed storage in a transmission network," IEEE Trans. Power Syst. **30**, 2288–2300 (2015).
[16]M. Ghofrani, A. Arabali, M. Etezadi-Amoli, and M. S. Fadali, "Energy storage application for performance enhancement of wind integration," IEEE Trans. Power Syst. **28**, 4803–4811 (2013).
[17]M. Zidar, P. S. Georgilakis, N. D. Hatziargyriou, T. Capuder, and D. Skrlec, "Review of energy storage allocation in power distribution networks: Applications, methods and future research," IET Gener. Transm. Distrib. **10**, 645–652 (2016).
[18]J. Y. Moon and J. Park, "Smart production scheduling with time-dependent and machine-dependent electricity cost by considering distributed energy resources and energy storage," Int. J. Prod. Res. **52**, 3922–3939 (2014).
[19]C. C. Chu and H. H. C. Iu, "Complex networks theory for modern smart grid applications: A survey," IEEE Trans. Emerg. Sel. Top. Circuits Syst. **7**, 177–191 (2017).
[20]E. Bompard, D. Wu, and F. Xue, "Structural vulnerability of power systems: A topological approach," Electr. Power Syst. Res. **81**, 1334–1340 (2011).
[21]S. W. Mei, F. He, X. M. Zhang, S. Y. Wu, and G. Wang, "An improved opa model and blackout risk assessment," IEEE Trans. Power Syst. **24**, 814–823 (2009).
[22]E. Bompard, R. Napoli, and F. Xue, "Extended topological approach for the assessment of structural vulnerability in transmission networks," IET Gener. Transm. Distrib. **4**, 716–724 (2010).
[23]V. Latora and M. Marchiori, "Efficient behavior of small-world networks," Phys. Rev. Lett. **87**, 198701 (2001).
[24]G. A. Pagani and M. Aiello, "From the grid to the smart grid, topologically," Phys. A **449**, 160–175 (2016).
[25]S. Arianos, E. Bompard, A. Carbone, and F. Xue, "Power grid vulnerability: A complex network approach," Chaos **19**, 013119 (2009).
[26]E. Bompard, R. Napoli, and F. Xue, "Analysis of structural vulnerabilities in power transmission grids," Int. J. Crit. Infrastruct. Prot. **2**, 5–12 (2009).
[27]H. Ronellenfitsch, M. Timme, and D. Witthaut, "A dual method for computing power transfer distribution factors," IEEE Trans. Power Syst. **32**, 1007–1015 (2017).
[28]M. Papadimitrakis, N. Giamarelos, M. Stogiannos, E. Zois, N.-I. Livanos, and A. Alexandridis, "Metaheuristic search in smart grid: A review with emphasis on planning, scheduling and power flow optimization applications," Renewable Sustainable Energy Rev. **145**, 111072 (2021).
[29]Sarjiya, A. B. Mulyawan, A. Setiawan, and A. Sudiarso, "Thermal unit commitment solution using genetic algorithm combined with the principle of tabu search and priority list method," in *2013 International Conference on Information Technology and Electrical Engineering (ICITEE)* (IEEE, 2013), pp. 414–419.
[30]R. D. Zimmerman, C. E. Murillo-Sanchez, and R. J. Thomas, "Matpower: Steady-state operations, planning, and analysis tools for power systems research and education," IEEE Trans. Power Syst. **26**, 12–19 (2011).
[31]K. Zou, A. P. Agalgaonkar, K. M. Muttaqi, and S. Perera, "Distribution system planning with incorporating dg reactive capability and system uncertainties," IEEE Trans. Sustainable Energy **3**, 112–123 (2012).
[32]IEEE Committee Report, "IEEE reliability test system," IEEE Trans. Power Appar. Syst. **98**, 2047–2054 (1979).
[33]IEEE, see http://labs.ece.uw.edu/pstca/pf300/pg_tca300bus.htm for "300 bus power flow test case" (1993).